Sound Absorption Effects in a Rectangular Enclosure with the Foamed Aluminum Sheet Absorber

Jae-Eung Oh*, Sang-Hun Kim, Jin-Tai Chung* and Kyung-Ryul Chung*****

(*Received December 5, 1997*)

For the purpose of finding out the optimal thickness of sound absorber and the sound absorption effects due to the selected thickness at an interested frequency range, the analytical study identifies the interior and exterior sound field characteristics of a rectangular enclosure with foamed aluminum lining and the experimental verification is performed with random noise input. By using a two-microphone impedance tube, we measure experimentally the absorption coefficient and the impedance of simple sound absorbing materials. Measured acoustical parameters of the test samples are applied to the theoretical analysis to predict sound pressure field in the cavity. The sound absorption effects from measurements are compared to predicted ones in both cases with and without foamed aluminum lining in the cavity of the rectangular enclosure.

Key Words: Absorption Coefficient, Admittance, Foamed Aluminum Sheet Absorber, Normalized Impedance, Porous Sound Absorber, Sound Radiation

1. Introduction

Sound absorbing materials have been widely used in noise control engineering such as vehicle compartments, machinery, building constructions, etc.

Until now, engineers have tried to develop the quantitative acoustical design with the trial-and-error method. To improve the acoustical performance of sound absorbing materials, the surface impedance and the absorption coefficient of absorbing materials should be identified before the acoustical design is accomplished. These acoustical parameters allow the quantitative design of sound absorbing configurations on the basis of materials and geometric parameters. (Cremer & Heckl, 1988; Reynolds, 1981: Beranek & Ver, 1992) Sponges and glass fibers, which have widely used for many years, have some difficulties in use. The composition of traditional materials would be dispersed due to long-time use; moreover, the absorbing performance would be worse in wet condition. On the other hand, the foamed aluminum is robust for dispersion and wetness, and its performance even in high temperature is very excellent. Foamed aluminum is well known metallic porous sound absorption material, which has excellent properties of lightweight and high acoustical absorption performances.

The past researches for the porous materials have studied on the sound propagation and the sound transmission through a medium. In most cases, the sound propagation through the porous layers has been calculated using a simplified analytical theory. The acoustical characteristics of metallic porous material have been studied since the research of Beranek and Biot in 1950's. Biot described the propagation of elastic waves

* Department of Mechanical Engineering, Hanyang University, 17, Haengdang Dong, SungDong Gu, Seoul 133-791, Korea

** Structural Analysis Team, Korea Testing Laboratory 222-13, Guro 3 Dong, Guro Ku, Seoul 133-791, Korea

*** High Speed Train Technology R&D Division, Korea Institute of Industrial Technology, San 17-1, Hong-Chon Ri, IbJang Myun, ChonAn Si 330-820, Korea

through a fluid filled porous medium in his research. In recent days, new models for the transmission of sound through layered systems containing porous materials are presented. Lauriks et al. (1992) and Rebilland et al. (1992) described the sound propagation through the porous material using a matrix representation of the layer obtained from the Biot theory. In 1996, Park applied Allard's modelling method that employs the method of acoustic transfer matrix (ATM) to yield more precise results in the analysis of porous sound absorbing materials. Experimental studies and simple applications on the sound absorption effects in space with porous materials have been performed since 1980's. The researches using foamed aluminum has been expanded since middle of 1980's. Akiyama et al. (1991) reported the acoustical characteristics and simple applications to the industry of foamed aluminum. They presented the foamed aluminum had better sound absorption effect than the common glass wool fiber and their simple applications verified the capability to actually apply the foamed aluminum

Based on the acoustical characteristics and the capability described in the previous researches, this study concentrates on identification of sound absorption effects due to the foamed aluminum sheet absorber, comparing the analytical and experimental methods. This study investigates the interior and exterior sound field characteristics of an acoustically loaded rectangular enclosure. The sound pressure field is identified by analysis adding the acoustical damping and reactivity of the absorbing material at the wall to the an analysis of the rigid walled enclosure. The optimal thickness of the sheet absorber can also be obtained by using the complex admittance at the absorber surface. Sound absorbers used in this study consist of one sponge, recycled rubber sheet from waste tire, and foamed aluminum sheet. Recycled rubber absorbers are made of small rubber pieces, which have different porous sizes for the size and density of rubber piece. The sound absorption coefficients and normalized impedance of the sample absorbers are measured and they are used in the theoretical analysis. The sound attenuation effects in and out of the cavity due to the foamed aluminum sheet absorber are verified with analytical and experimental studies when the foamed aluminum absorber covers the bottom of the enclosure.

2. Sound Pressure Field in the Rectangular Enclosure with a Lightly Damped Wall

The sound pressure field by an imposed vibration of the enclosure walls is determined by using the Green function $G(\boldsymbol{x} \mid \boldsymbol{y})$, which is defined as the sound pressure at point $\boldsymbol{x}$ in the cavity due to a unit sound at point $\boldsymbol{y}$. The sound pressure at point $\boldsymbol{x}$ in the cavity could be expressed as sum of a series of acoustic modes in the enclosure. The dimensions of the enclosure used in this study are given by the x_1, x_2, x_3 co-ordinates, as shown in Figure 1.

This Green function for the enclosure satisfies

$$(\nabla^2 + k^2) G(x|y) = -\delta(x-y) \tag{1}$$

where, $k=\omega/c$ and therefore quantifies the spatial dependence of the complex pressure field produced in the enclosure by a point source at position $\boldsymbol{y}$. The Green function is determined in terms of the rigid walled eigenfunctions of the enclosure such that the Green function also satisfies rigid walled boundary conditions i. e. $\nabla G(x|y) \cdot n=0$, where $\boldsymbol{n}$ is the unit vector pointing out of the volume on its surface. Thus we assume that

$$G(x|y) = \sum_{m=0}^{\infty} b_m \Psi_m(x) \tag{2}$$

where b_m are complex coefficients that have to be

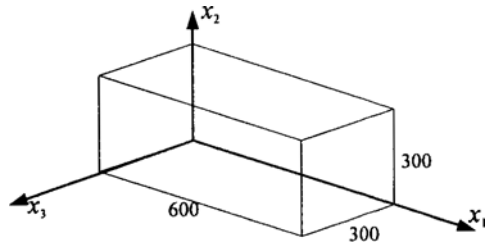

Fig. 1 The co-ordinate system and definitions of the enclosure dimensions.

determined and these coefficients depend on the source position $\boldsymbol{y}$. Since the eigenfunctions $\Psi_m(x)$ form a set of bases for a finite-dimensional function space, a function of $\boldsymbol{x}$ can be expanded by linear combination of the eigenfunctions. The expansion is analogous to the half period Fourier series expansion of a wave form. Substitution of Eq. (2) into Eq. (1), with $\nabla^2\Psi_m(x) = -k_m^2\Psi_m(x)$, yields

$$\sum_{m=0}^{\infty} b_m(k^2-k_m^2)\,\Psi_m(x) = -\delta(x-y) \tag{3}$$

where, k_m^2 is the eigenvalue corresponding to the eigenfunction $\Psi_m(x)$. Multiplying both sides of Eq. (3) by $\Psi_n(x)$, and then integrating both sides over the volume V of the enclosure, and then applying the orthonomality of the eigenfunctions and the shifting property of three-dimensional Dirac delta function, the Green function $G(\boldsymbol{x} \mid \boldsymbol{y})$ can be rewritten as

$$G(x|y) = \sum_{n=0}^{\infty} \frac{\Psi_n(x)\,\Psi_n(y)}{V(k_n^2-k^2)} \tag{4}$$

The sound pressure field in the enclosure is derived by using the general solution to the Helmholtz equation :

$$p(x) = (-)\iint\{G(x|y)\,\mathrm{grad}\,p(y) - p(x)\,\mathrm{grad}\,G(x|y)\}\cdot dS + \iint\rho(y)\,G(x|y)\,dV \tag{5}$$

Since the Green function satisfies rigid walled boundary conditions in case of no "volume" source within the enclosure, the sound pressure field can be expressed as

$$p(x) = \int_S G(x|y)\nabla_y p(y)\cdot \mathrm{n}\cdot dS \tag{6}$$

where the pressure gradient on the enclosure walls $\nabla_y p(y)$ can occur due to two mechanisms. The first one is the imposed surface normal vibration $u_i(\boldsymbol{y})\mathbf{n}$ and the second one is the surface normal particle velocity resulting from the finite impedance of the enclosure walls.

Consider the boundary conditions on the surface of the enclosure. This study analyzes the non-rigid enclosure which has locally reacting surfaces. The locally reacting surface can not have the wave motion within the walls of the enclosure; therefore, the boundary condition at each point on the surface S can be described, for a harmonic sound field, in terms of its specific acoustic impedance $z(\boldsymbol{y})$ at that point:

$$\frac{p(y)}{u(y)} = z(y) \text{ on } S \tag{7}$$

where $u(\boldsymbol{y})$ is the complex acoustic particle velocity normal to the surface at position $\boldsymbol{y}$ on the surface of the enclosure.

Assuming the harmonic excitation of the enclosure with frequency ω, the particle velocity can be expressed in terms of derivatives of complex pressure acting in the direction normal to and into the wall. Using the momentum equation, it follows that

$$\nabla p(y)\cdot n = -j\omega\rho u(y) \tag{8}$$

where ρ is the acoustic density of air. The normalized specific acoustic admittance $\beta(\boldsymbol{y})$ of the wall at position $\boldsymbol{y}$ is defined as

$$\beta(y) = \frac{\rho c}{z(y)} = \chi(y) + j\sigma(y) \tag{9}$$

where c is the sound speed and the real and imaginary parts of $\beta(\boldsymbol{y})$ are the normalized specific acoustic conductance $\chi(\boldsymbol{y})$ and normalized specific acoustic susceptance $\sigma(\boldsymbol{y})$, respectively. The homogeneous boundary condition on the surface can now be expressed as

$$\nabla p(y)\cdot \mathrm{n} = -jk\beta(y)\,p(y) \text{ on } S \tag{10}$$

Now we can describe the sound pressure field in enclosure whose surfaces have a small value of $\beta(y)$ and boundary conditions given by Eq. (10) by using the rigid walled eigenfunctions $\Psi_n(x)$. We use Eq. (10) to describe the surface normal particle velocity resulting from the finite impedance of the enclosure walls. Substitution of Eqs. (8) and (10) into Eq. (6) leads to

$$p(x) = \int_S [j\omega\rho u_i(y)\cdot \mathrm{n} - jk\beta(y)\,p(y)]\,dS \tag{11}$$

As described in Eq. (6), the pressure $p(\boldsymbol{x})$ is dependent not only on the prescribed surface velocity $u_i(\boldsymbol{y})$ but also on the sound pressure $p(\boldsymbol{y})$ on the enclosure walls. We now show that we can make an approximation that enables the sound pressure field to be expressed in terms of a

series of damped modal responses, where the second term in the square brackets of Eq. (11) is seen to be directly responsible for this damping mechanism. First, the series expansion for the Green function given by Eq. (4) shows that Eq. (11) can be written as

$$p(x)=\sum_{n=0}^{\infty} a_n \Psi_n(x) \tag{12}$$

where the coefficients an are given by

$$a_n=\frac{1}{V(k_n^2-k^2)}\left[\int_S j\omega\rho\Psi_n(y)\,u_1(y)\cdot n\cdot dS - \int_S j\omega\rho\Psi_n(y)\,\beta(y)\,\rho(y)\cdot dS\right] \tag{13}$$

3. Measurement of Absorption Coefficients and Normalized Impedance

The experimental setup to measure the absorption coefficients and normalized impedance of absorbing materials is shown in Fig. 2. A two-microphone impedance measurement tube (B&K type 4206) is used to measure the acoustic absorption coefficients and normalized impedances of test samples and it is controlled by a multi-channel analysis system (B&K type 3550). The analyzer generates random signals, which are amplified by a power amplifier (B&K type 2706). The response signals from the two microphones are analyzed by the analysis system that calculates the acoustic absorption coefficient and normalized impedance. The samples used in the test are shown in Fig. 3.

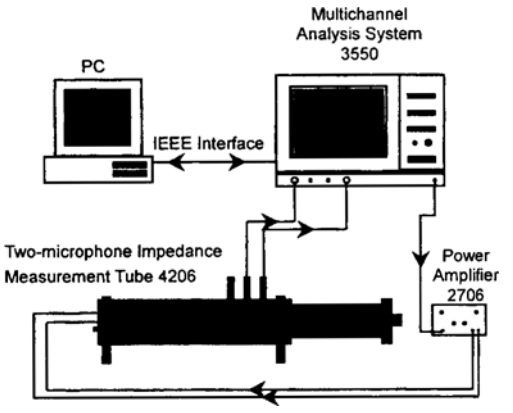

Fig. 2 Experimental setup to measure the absorption coefficient and the normalized impedance.

Consider the absorption coefficient and normalized impedance experimentally measured for the sponge, the recycled rubber sheet, and the foamed aluminum sheet. The absorption coefficients and the normalized impedance of the porous material are dependent upon the friction between air particles and the porous surfaces. The friction results in energy loss in proportion to the air particle velocity that increases with the frequency. Generally the big pores and the irregular surface of the foamed aluminum are helpful to make the absorption coefficients higher, because they increase interference between sound waves and the wall surfaces. Figure 4 shows the absorption coefficient of the test samples with 24mm in thickness. The sponge has relatively low absorption coefficients in all the frequencies, while the recycled rubbers have higher absorption coefficients than the sponge. The foamed aluminum shows the best absorption performance in the range of 400Hz to 1200Hz, which is interested frequency range in this study. The maximum absorption coefficient is shown around 800Hz. Since most of the structural-acoustic coupled systems have acoustical natural frequencies below 1500Hz, it seems that the foamed aluminum sheet

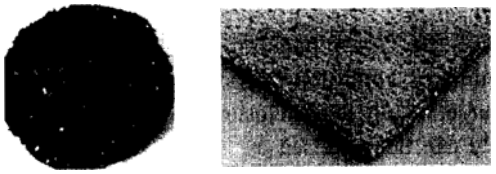

(a) Recycled rubber (b) Foamed aluminum

Fig. 3 Surface of the test samples.

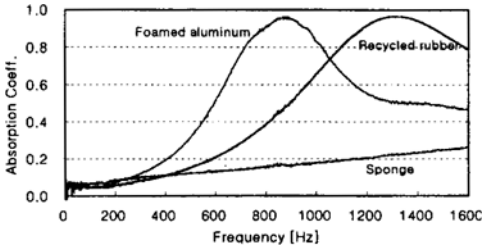

Fig. 4 Measured absorption coefficent of the test samples.

absorber has prominent sound absorption performances in the interested frequency range.

4. Prediction of Interior Sound Pressure of the Enclosure with Different Impedance

The sound pressure field is analyzed in the rectangular cavity with rigid walls when the foamed aluminum sheet absorber covers the bottom of the enclosure. We consider the enclosure with the size of $600\times300\times300$ mm. Since the sound pressure is closely related with the admittance which is defined as the inverse of the impedance at an absorber surface, the predicted pressure can be obtained by using the complex formulas given by Eq. (12). The complex admittance in the equation is calculated from the measured impedance of the test sample. The real and imaginary parts of the admittance in Figs. 5 and 6 are plotted for different thicknesses of the foamed aluminum sheet absorber, respectively.

An interesting fact can be seen in the relation between the admittance and the sound pressure in the frequency domain. The real part of the admittance is related with the sound attenuation of the resonant peaks, while the imaginary part is related with the frequency shift of the resonant peaks. Consequently, the real part of the admittance controls the amplitudes of the resonant peaks. In other words, increasing the real part reduces significantly the amplitude of the peaks at the natural frequencies, because the real part represents damping, i. e. , air resistance of sound at the wall. Hence, noise can be reduced by controlling the real part.

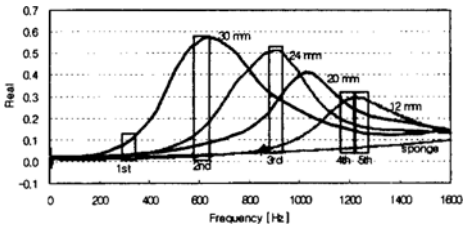

Fig. 5 Real part value curves of admittance for the different thickness of foamed aluminum.

The optimal thickness of the sheet absorber can be obtained by using the complex admittance at the absorber surface. Figure. 5 shows the real part value curves of admittance for the thicknesses of 12mm, 20mm, 24mm and 30mm. The more the thickness increases, the more the peak of real value increases and shifts to lower frequency. Figure 6 shows that the turn-over point of the imaginary shifts to the low frequency as thickness increases. The predicted sound pressure attenuation at each resonant frequency is displayed in Fig. 7 for different thicknesses of the foamed aluminum sheet. As shown in Fig. 7, it is difficult to reduce the amplitude of fundamental acoustical natural frequency by using the absorber. This result shows the low frequency criteria of the sound absorber. The sound absorber affects the frequency range over 300~400Hz. In order to reduce the sound pressure in the frequency range of 500~1200Hz, in which structural-acoustic coupled structure used in this cavity has dominant frequency characteristics, the absorber should have maximum absorption performance in the frequency range including 2nd, 3rd, and 4th resonance peaks. It can be seen that the optimal

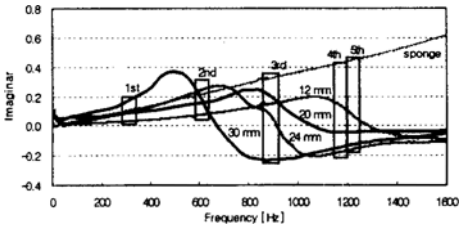

Fig. 6 Imabinary part value curves of admittance for the different thickness of foamed aluminum.

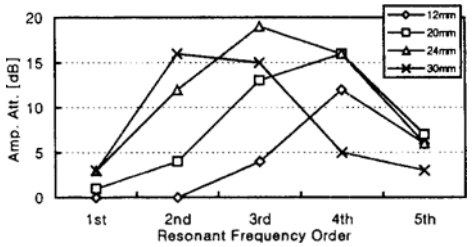

Fig. 7 Predicted sound pressure attenuation at each resonance peak according to the different thickness of foamed aluminum absorber.

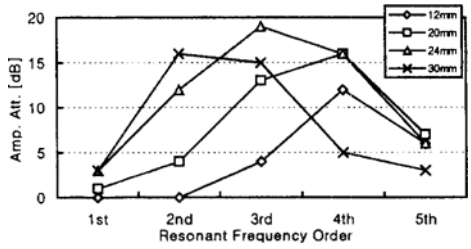

Fig. 8 Predicted sound pressure curves according to the different thickness of foamed aluminum absorber.

thickness of the sheet absorber is 24mm. Figure 8 shows the predicted sound pressure curves according to the thickness of the foamed aluminum sheet absorber. The 12mm sheet absorber affects only the 4th and 5th resonance peaks and the 24mm absorber has large sound attenuation in the frequency range of 400~1200Hz, especially over 2nd resonance peak.

5. Sound Absorption Effects in the Cavity with Foamed Aluminum Lining

To verify the theoretical model for the sound pressure in the rectangular enclosure, predicted sound pressure levels are compared with the measured sound pressure levels. The sound pressure is measured by using the acoustical excitation with the white noise, while the predicted sound pressure level is computed by assuming velocity excitation. The sound absorption effects, which are necessary for computation, are obtained from the sound pressure response when the sound absorber with known impedance (foamed aluminum) covers the bottom of the enclosure. For both measurement and prediction, a constant volume-velocity source is used, which is on the wall of the rectangular enclosure with dimensions $600\times300\times300$ mm. The source is located at (0, 150mm, 150mm) and the interior microphones are located at P1 (130mm, 150mm, 95mm), P2 (200mm, 150mm, 150mm), P3 (300mm, 210mm, 90mm) and P4 (450mm, 90mm, 220mm).

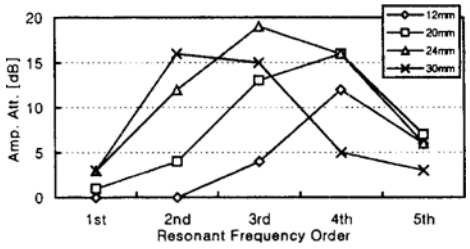

(a) P2 position (200mm, 150mm, 150mm)

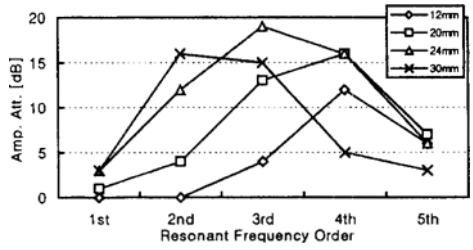

(b) P3 position (300mm, 210mm, 90mm)

Fig. 9 Predicted versus measured sound pressure curves in a cavity without absorber.

Consider first the sound pressure in the enclosure without the absorber: the cavity has undamped rigid walls. The predicted and measured sound pressure curves are shown in Fig. 9, where the resonance peaks resulting from excitation of volume velocity (speaker) are identified. Figure 9 shows that the measured acoustical natural frequencies coincide closely with the predicted ones. However, the predicted sound pressure levels are slightly higher than the measured levels. Theoretically, the response should be infinite at resonance for an undamped, rigid-wall enclosure. In practice, however, damping is present even for an enclosure with very rigid walls, because viscous and thermal losses occur in the air and at the boundaries. Actually the walls of the enclosure in the experiment, which is made of acrylic, have much lower impedance values than theoretical rigid-walls. In this study, the impedance of walls without the absorber is assumed as 10^7.

Next, the sound pressure is investigated for the rectangular cavity with the foamed aluminum

sheet absorber at the bottom wall side only. The complex admittance of the absorber characterizes the sound attenuation effect in the cavity. Figure 10 compares the predicted and measured sound pressure levels in case that the bottom wall is covered with foamed aluminum. The figure shows that the measured acoustical natural frequencies coincide closely with the predicted ones for the lightly damped wall cavity. The predicted response shows that the level is attenuated over 10dB at resonance frequency each due to the foamed aluminum and has dominant peaks at the resonance frequencies. In practice, the measured sound pressure level curve shows much amount of sound attenuation which makes the peaks blunt in the frequency range of 500~1200Hz. The

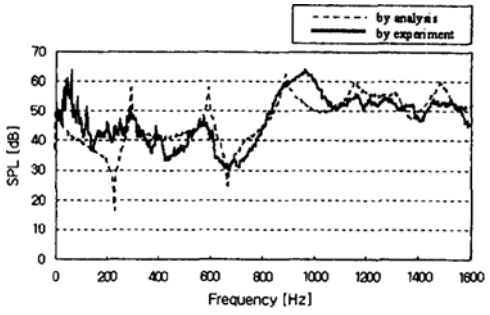

(a) P1 position (130mm, 150mm, 95mm)

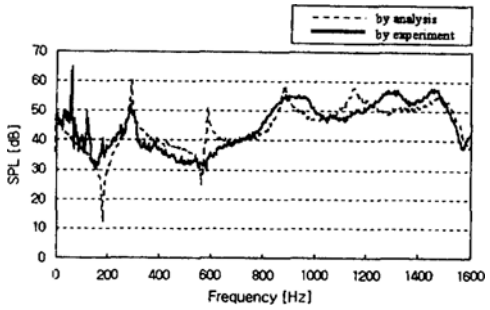

(b) P2 position (200mm, 150mm, 150mm)

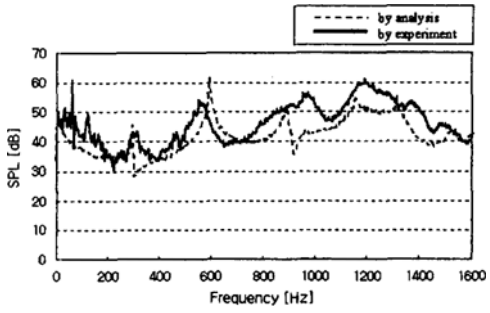

(c) P3 position (300mm, 210mm, 90mm)

Fig. 10 Predicted vs. measured sound pressure curves when foamed aluminum covers bottom of cavity.

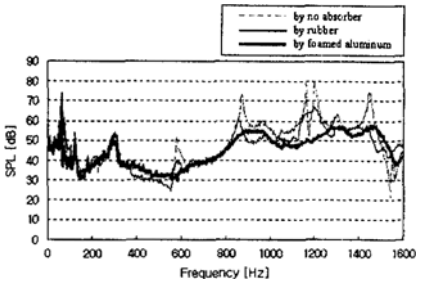

(a) P1 position (130mm, 150mm, 95mm)

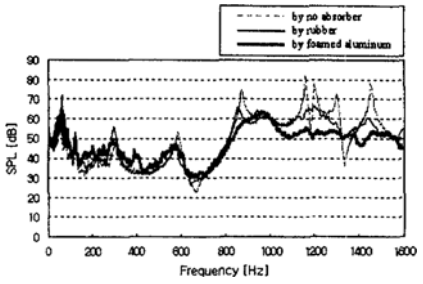

(b) P2 position (200mm, 150mm, 150mm)

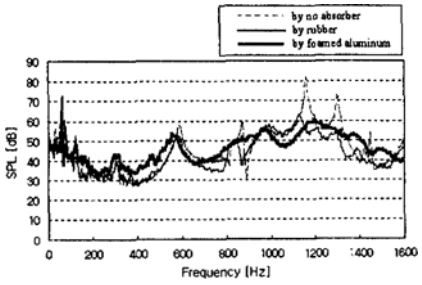

(c) P3 position (300mm, 210mm, 90mm)

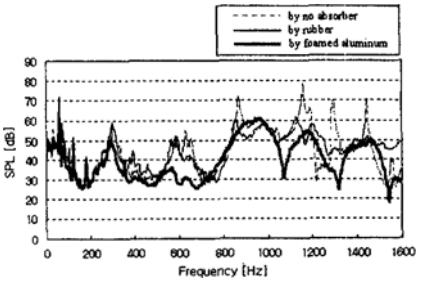

(d) P4 position (450mm, 90mm, 220mm)

Fig. 11 Measured sound absorption effects of the interior noise.

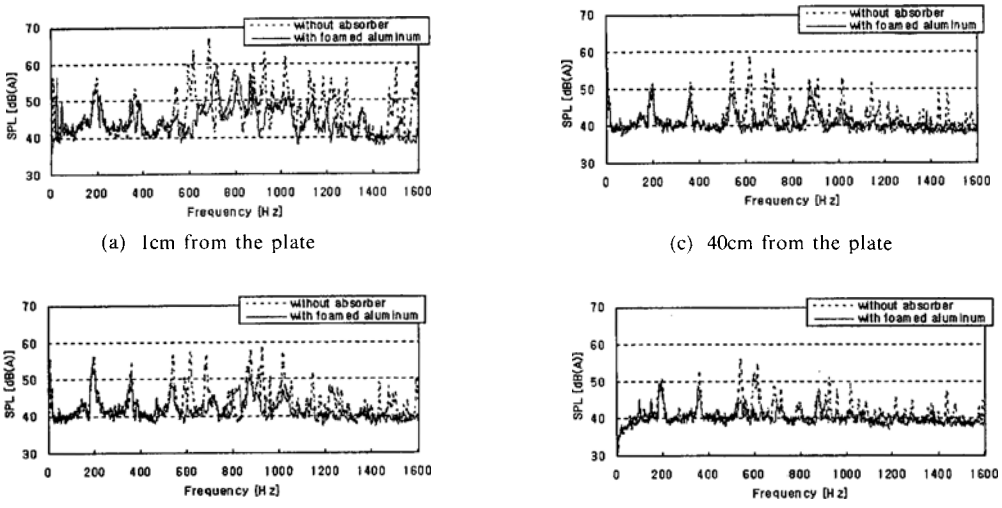

(a) 1cm from the plate

(c) 40cm from the plate

(b) 20cm from the plate

(d) 70cm from the plate

Fig. 12 Measured sound absorption effects of the exterior noise.

characteristics in the low frequency range under 400Hz shows that the foamed aluminum does not affect sound attenuation significantly in practice.

The measured sound absorption performance of the foamed aluminum is displayed in Fig. 11, which is compared with the recycled rubber and undamped wall. Figure 11 shows the results of the measured sound absorption effect by comparing the sound pressure level curves in the rigid wall cavity. In the case that the recycled rubber covers the bottom of the enclosure, the sound pressure curve shows a sound attenuation by about 10dB and dominant peak at resonance frequencies. Experimental results for the foamed aluminum show a significant effect on the noise attenuation above the fundamental acoustical natural frequency. The measurement results show over 20dB difference in noise reduction at each acoustical natural frequency.

6. Exterior Sound Attenuation Effect Due to the Inner Foamed Aluminum Lining

The analytical and experimental verification in the rigid walled cavity leads to the prediction of radiated sound throughout the flexible steel plate of a structural-acoustic coupled enclosure. For free and/or far field, the exterior sound pressure field depends at the acoustical modal response on high frequencies. The measurement of sound pressure in the outer field of the enclosure is performed at 1~70cm distance from the plate. The measured sound pressure curves at different distances for both with and without the foamed aluminum lining in the cavity are displayed in Fig. 12. Experimental result at 40cm from the plate due to the foamed aluminum in the cavity shows that the sound attenuation of the resonant peaks is evident to the frequency range above 500Hz and the measurement results shows over 15dB(A) difference at each resonance peaks.

7. Conclusions

The selection of optimal thickness and the sound attenuation effects of interior and exterior field due to the foamed aluminum sheet absorber are investigated by the analytical and experimental approaches. The traditional sound absorbers have been made for their absorbing performance to fit to high frequency range of 1~4kHz. On the other hand, the recycled rubber and the foamed aluminum, which are developed recently, have large absorption coefficient in low frequency range. Throughout the measurement in this study, it can be seen that the recycled rubber has high

absorption coefficient in the frequency range of 1000~1600Hz and the foamed aluminum has maximum value in 400-1200Hz. Because the natural frequencies of a structural-acoustic coupled structure, which is used in this study, are presented in the range below 1500Hz, it can be seen easily that the foamed aluminum maximize the sound attenuation effect in the interested frequency range.

This study puts a focus on the selection of thickness that has the maximum sound attenuation effect in the interested frequency range. To determine the optimal thickness of the foamed aluminum sheet absorber that makes the best effect in the cavity, theoretical method used the admittance at the wall surface. The optimal thickness of sheet absorber for the reduction of sound pressure in this enclosure was 24mm.

In order to verify the theoretical result, predicted sound pressure levels obtained from the theoretical model are compared with measured sound pressure levels when the 24mm foamed aluminum covers the bottom of cavity. Experimental result due to the foamed aluminum showed a significant effect on the attenuation of the interior and exterior noise above the fundamental natural frequency. In the interior sound field, the measurement resultes showed over 20dB difference in noise reduction at each acoustical natural frequency. At 40~50cm distance from the plate, the exterior noise was reduced by over 15dB(A) at resonance peaks.

References

Cremer, L. and Heckl, M., 1988, *Structure -Borne Sound,* Springer-Verlag Berlin

Douglas D. Reynolds, 1981, *Engineering Principles of Acoustics,* Allyn and Bacon, Inc.

Leo L. Beranek and Istvan L. Ver, 1992, *Noise and Vibration Control Engineering,* John Wiley and Sons, Inc.

M. A. Biot, 1956, "Theory of Propagation of Elastic Waves in a Fluid-Saturated Porous Solid," *Journal of the Acoustical Society of America,* Vol. 28, No. 2, pp. 168~178

W. Lauriks, P. Mees and J. F. Allard, 1992, "The Acoustic Transmission Through Layered Systems," *Journal of Sound and Vibration,* Vol. 155, No. 1, pp. 125~132

Rebillard, P., Allard, J. F., Depollier, C., Guignouard, P., Lauriks, W., Verhaegen C., and Cops, A., 1992, "The Effect of a Porous Facing on the Impedance and the Absorption Coefficient of a Layer of Porous Material," *Journal of Sound and Vibration,* Vol. 156, No. 3, pp. 541~555

Akiyama, S., Itoh M., and Ishii, E., 1991, "Sound effects of foamed aluminum," *Government Industrial Research Institute,* Kyushu, Report No. 46

Park, C. H., Joo J. M., and Yom, C. H., 1996, "A study on the acoustic properties of porous material by using acoustic transfer matrix," *Journal of KSNVE,* Vol. 6, No. 5, pp. 635~644